Materials Advances

ROYAL SOCIETY OF CHEMISTRY

PAPER

View Article Online
View Journal | View Issue

Cite this: *Mater. Adv.*, 2025, **6**, 1788

Memristive behaviour of PANI/Au hybrid nanocomposites synthesized *via* various routes†

Aldobenedetto Zotti, ‡[a] Salvatore Aprano,‡[b] Asma Rafiq,[c] Simona Zuppolini, *[a] Mauro Zarrelli,[a] Maria Grazia Maglione,[b] Paolo Tassini, [b] Antonio Cassinese[c] and Anna Borriello[a]

Received 9th December 2024,
Accepted 5th February 2025

DOI: 10.1039/d4ma01218f

rsc.li/materials-advances

Herein, hybrid nanocomposite devices based on polyaniline (PANI) nanofibers decorated with gold nanoparticles (Au), as conductive fillers, and atactic polystyrene (aPS), as insulating matrix, were developed. To assess the effect of the PANI and Au synthesis procedure on the electrical behavior of the developed devices, PANI/Au nanosystems were synthesized *via* two different routes: (1) biphasic synthesis, wherein PANI nanofibers were grown through a biphasic synthesis procedure incorporating 1-dodecanthiol-capped Au (AuDT) nanoparticles, which were previously synthesized and dispersed in the reaction environment; (2) one-pot synthesis, wherein gold nanoparticles were directly reduced, starting with auric salt precursors on the PANI nanofiber surface, which were previously synthesized *via* a rapid mixing procedure. Thermal stability and the Au/PANI weight ratio were determined using thermogravimetric analysis (TGA). Furthermore, PANI/Au nanosystems were observed using transmission electron microscopy (TEM), revealing that the synthesis route significantly affected the morphology of nanosystems. Electrical characterization showed that aPS/PANI/Au hybrid nanocomposite devices exhibited a typical non-linear current–voltage curve with a closed hysteresis loop, which is a characteristic of memristive behavior. Moreover, devices made with fibers obtained *via* rapid mixing (PANI RM/Au) exhibited conductivities higher than those produced with fibers from biphasic synthesis (PANI BF/AuDT).

1. Introduction

Semiconductor technology has promoted a rapid and radical advancement in information processing through the development of high-speed and -density non-volatile memory devices. Further progression in the memory technology field requires nanoscale device development, among which the two-terminal electronic device architecture turns out to be the most promising since overall device dimensions only depend on electrode sizes. Nanomaterials such as donor–acceptor charge-transfer complexes,[1] bistable molecules,[2] and nanocomposites comprising organic materials and metal nanoparticles[3,4] are suitable for incorporation into a memory device architecture. Among the organic materials, inherently conducting polymers (ICPs), including polyanilines (PANIs), polythiophenes (PTs) and polypyrroles (PPys), are particularly suitable for the development of electronic devices owing to their electrical properties comparable to those of inorganic materials (semiconductors and metals).[5] Moreover, ICPs can potentially replace many of these materials owing to their lower manufacturing costs, lower density, better processability, higher mechanical flexibility and broader chemical functionalization capabilities. Furthermore, owing to the minimal thermal expansion coefficient and mechanical property mismatch between ICPs and structural polymers, the development of stable conductive plastic composite components is a concrete possibility.[5]

Polyaniline (PANI) is one of the most important ICPs with the potential for a multitude of applications, especially in chemical sensors and electronic devices.[6] Within the ICPs family, PANI is unique owing to its ease of synthesis, environmental stability, and reversible conductivity achieved by doping/de-doping. PANI can be synthesized by both chemical oxidation and electrochemical polymerization of the aniline monomer under mild conditions.[7] PANI can be found in three different oxidative states, *i.e.* pernigraniline, leucoemeraldine and emeraldine base. In the latter state, PANI becomes electrically conductive when doped with acids as it will form the emeraldine salt form. The electrical conductivity of PANI can be reversibly varied, from 10^{-10} S cm^{-1} (for the undoped insulating base form) to 1 S cm^{-1} (for the fully doped conducting salt

[a] *Institute for Polymers, Composites and Biomaterials, National Research Council, P.le Fermi, 1, 80055 Portici, Naples, Italy. E-mail: simona.zuppolini@cnr.it*
[b] *Portici Research Center, ENEA, Piazzale Enrico Fermi 1, 80055 Naples, Italy*
[c] *Physics Department and INFN-Napoli, Università Napoli Federico II, P.le Tecchio 80, 80125 Naples, Italy*

† Electronic supplementary information (ESI) available. https://doi.org/10.1039/d4ma01218f

‡ These authors contributed equally.

form). In recent years, the synthesis and applications of PANI nanostructures have been popular topics in research. PANI nanofibers have been deeply studied owing to the intrinsic one-dimensional structures of the rigid PANI macromolecule,[8] and compared to other morphologies, nanofibers show better suspension ability and larger surface areas that guarantee improved performances for applications such as memory devices and chemical sensors.[9]

Metal nanoparticles, such as silver and gold, have been extensively studied due to their unique optical properties.[10] Thus, PANI/noble metal nanoparticle composites have gained considerable attention due to their long-term solution stability, nanoparticle size tunability and possible use in chemical sensors, catalyst development and memory devices.[11] In particular, one of the main features that a memory device should possess is memristive behaviour, *i.e.*, a bi-stable electrical conductivity depending on the applied voltage history to reproduce the 0/1 states.[12]

PANI nanofibers can be fabricated using different synthetic routes such as electrospinning,[13] hard templates,[14] soft templates,[15] interfacial polymerization[16] and seeding polymerization.[17] Among these, polymerization assisted by hard templates (carbon nanotubes, graphite, and inorganic oxides) is mainly used for PANI synthesis,[18] especially for developing sensors and energy storage devices. Milakin *et al.*,[19] for example, developed ascorbic acid sensors based on the PANI growth on a hard template of a carbon black paste, while Xia *et al.*[20] reported the growth of ordered whisker-like polyaniline on the surface of a mesoporous carbon template as well as its excellent supercapacitor properties. On the other hand, interfacial polymerization has achieved considerable attention due to the possibility of producing high-quality PANI nanofibers by controlling their morphology, size and diameter,[21] following simple procedures, and allowing a wide choice of solvent pairs, acid dopants, and reagent concentrations over a broad range of temperatures. Pillalamarri *et al.*[22] used a one-pot synthesis method in which composite materials consisting of PANI nanofibers decorated with noble-metal (Ag or Au) nanoparticles were synthesized by γ-radiolysis. Sarma *et al.*[23] have prepared PANI-gold nanocomposites by first reducing the gold salt solution and then polymerizing aniline in the same medium. PANI nanofibers decorated with gold nanoparticles were synthesized by Tsang *et al.*[24] devices built incorporating these hybrid fibers within a polyvinyl alcohol (PVA) matrix have shown a memristive behaviour, making this material a promising candidate as a digital memory device. Nevertheless, aggregation and overgrowth of noble metal nanoparticles on the PANI surface are commonly observed due to the lack of effective protection ability, and therefore, noble metal nanoparticle size control results are limited. So, there are still some fundamental aspects that must be analysed, such as the PANI synthetic route and the use of capping molecules to protect metal particles.

In this study, conductive hybrid composites comprising doped PANI fibers, with gold nanoparticles (Au NPs) as the conductive dispersed phase and atactic polystyrene (aPS) as the polymer matrix, were synthesized and characterized. Two distinct PANI/Au nanosystems were examined, obtained by exploiting different synthetic approaches for both PANI nanofibers and gold nanoparticles. In the first case, a nanocomposite system was obtained by the simultaneous incorporation of previously self-assembled 1-dodecanthiol-capped gold nanoparticles and PANI nanofiber formation at a biphasic interface (biphasic synthesis, BF). In the second case, gold nanoparticles were deposited on the PANI nanofibers, obtained by the rapid mixing synthesis method (RM), through the chemical reduction of gold salts. The influence of the synthesis route on the morphology and size of the PANI/Au nanosystem was examined, and the correlation between these parameters and the electrical characterization of the aPS/PANI/Au hybrid composites was performed. It was observed that the *I–V* curves show a memristor-like behaviour. The memristor-like behaviour observed in the *I–V* curves suggests potential applications in neuromorphic computing and memory devices. Further investigation into the mechanisms underlying this behaviour could provide valuable insights into the charge transport properties of these hybrid composites. Additionally, the study of different PANI/Au nanosystem synthesis routes opens possibilities for tailoring the electrical characteristics of the resulting composites for specific applications.

2. Experimental

2.1. Materials

Aniline, ammonium persulphate (APS), chloroauric acid ($HAuCl_4$), tetraoctylammonium bromide (TOAB), sodium borohydride ($NaBH_4$), 1-dodecanthiol (DT), camphor sulphonic acid (CSA), thioglycolic acid (TA), ammonium hydroxide, dodecyl benzene sulphonic acid (DBSA), carbon tetrachloride (CCl_4), atactic polystyrene (aPS, MW 280 000), chloroform ($CHCl_3$) and toluene were purchased from Sigma-Aldrich and used as received.

2.2. Synthesis of PANI BF/AuDT

The gold nanoparticles capped with 1-dodecanethiol (AuDT) were synthesized utilizing the two-phase arrested growth method.[25] 50 ml of $HAuCl_4$ solution (0.05 M) was poured into a separatory funnel along with 160 ml of TOAB in toluene solution (0.03 M). Upon complete separation of the biphasic system, the aqueous phase was removed, and DT (0.48 ml) was added to the organic phase and subjected to magnetic stirring for 10 min. Subsequently, 50 ml of $NaBH_4$ in an aqueous solution (0.4 M) was introduced dropwise to the toluene solution, and the system was allowed to react for 3 h and 30 min. The water/organic biphasic system was transferred to the separatory funnel, and the aqueous phase was removed. Toluene was removed using a rotary evaporator system set at 50 °C; finally, the as-prepared AuDT nanoparticles were collected using absolute ethanol, filtered, washed with acetone and dried in an oven under vacuum for 2 days.

The synthesized nanoparticles were utilised in the preparation of PANI BF/AuDT by an interfacial biphasic synthesis.[26] A solution comprising 20 mg of AuDT, 50 mg of DBSA (surfactant) and 47.41 g of CSA (dopant) in 200 ml of water was prepared

and sonicated for 2 h. Following the sonication stage, 1.27 g of APS (initiator) was added to the aqueous solution and gradually poured into a separatory funnel previously filled with 200 ml of aniline solution in carbon tetrachloride (0.1 M). After 10 h of the reaction, the organic phase was removed and the aqueous system was filtered, washed with bidistilled water and dried in an oven under vacuum at 80 °C for 24 h. The CSA-doped PANI nanofibers without gold nanoparticles were synthesized using the same procedure.

2.3. Synthesis of PANI RM/Au

PANI nanofibers were synthesized according to the ref. 27 aniline (0.6 ml) and APS (0.36 g) were dissolved in two vials containing 20 ml of HCl solution (1 M). These solutions were rapidly mixed, stirred for 30 s and allowed to react for 2 h at room temperature. The resulting greenish solution was filtered and washed with bidistilled water, and the filtrate was added to a 40 ml solution of ammonium hydroxide (0.1 M) for de-doping. After 0.5 h, the de-doped product was filtered again and dispersed in 40 ml of TA solution (0.1 M) for subsequent doping (0.5 h). The obtained PANI RM nanofibers were collected for the subsequent phase of gold reduction. In a typical gold nanoparticle deposition for gold reduction,[28] a precise amount of a 0.1 M $HAuCl_4$ solution was added to 50 ml of PANI RM nanofibers (2.0 g L^{-1}). According to ref. 29 TA is not capable of reducing $HAuCl_4$ without the presence of doped PANI, which acts as a reducing agent and conductive polymer at the same time. Two different $HAuCl_4$ concentrations were investigated: 1.8 mM and 0.36 mM. The system was kept under magnetic stirring for 2 h, and the product was filtered, washed and dried in an oven under vacuum at 80 °C for 24 h.

2.4. Characterization

Thermogravimetric analysis (TGA) was performed to evaluate the gold content in PANI/Au nanocomposites using a TGA Q500 system (TA Instrument, USA) under a nitrogen atmosphere (50 mL min^{-1}) and heating ramp of 10 °C min^{-1}. The sample weights were approximately 5 ± 0.5 mg, and the maximum temperature was 600 °C. The morphology of the PANI and PANI/Au hybrid composites was assessed using a bright field transmission electron microscopy (TEM) FEI Tecnai G12 Spirit Twin, equipped with a LaB6 source and a FEI Eagle 4k CCD camera (Eindhoven, The Netherlands) with samples, preliminary dispersed in chloroform and then deposited on a copper grid. The size distribution was assessed employing open-source Gwyddion software on TEM micrographs.

2.5. Device fabrication

The active layer of the developed devices consists of an atactic polystyrene (aPS) matrix incorporated within the synthesized polyaniline/gold (PANI/Au) hybrid nanofibers. To prepare this active layer, a solution of aPS in chloroform (1.6 wt%) was prepared at 60 °C under magnetic stirring and after the complete dissolution of the polymer had occurred, an appropriate amount of nanofibers (8.3 wt%) was added. The resulting system was ultrasonicated for 3 h with a sonication amplitude of 75 and a power of 40 W at ambient temperature. Prior to the deposition process, the glass substrates were meticulously cleaned using deionized water and detergent in an ultrasonic bath. This was followed by rinsing with acetone and isopropyl alcohol, and finally, drying in an oven at 120 °C for a minimum of 1 h. A silver contact was then formed on the glass substrates *via* thermal evaporation, conducted at a base pressure below 5×10^{-7} mbar with a deposition rate of approximately 2 Å s^{-1}. A shadow mask was used to achieve the desired pattern, specifically a strip measuring 1 mm in width. The solution was subsequently spin-coated onto the cleaned glass substrate by a Spin Coater 100 (CEE – Cost Effective Equipment, USA). The employed spin parameters included a spin velocity of 5000 rpm, spin acceleration of 1800 rpm, and spinning duration of 60 seconds, resulting in a deposited layer with an approximate thickness of 220 nm Finally, the silver counter electrode was evaporated onto the active layer under the same deposition conditions as those of the bottom contact, with the shadow mask oriented orthogonally to the bottom contacts. This configuration allowed the creation of a device with an active area of 1 mm^2.

3. Results and discussion

3.1. Synthesis of PANI/Au nanocomposites

PANI nanofibers were synthesized using two different approaches. In the biphasic synthesis (designated PANI BF), the monomer (aniline) and polymerization activator (APS) are dissolved in an organic phase (CCl_4) and water, respectively, with nanofibers growing at the phase interface while simultaneously incorporating previously self-assembled 1-dodecanthiol-capped gold nanoparticles (AuDT). In the rapid mixing synthesis (PANI RM), aniline and APS are directly dissolved and mixed in water, and subsequently, gold nanoparticles are deposited by the direct reduction of gold salts onto the surface of the attained doped PANI nanofibers. To assess the effect of the gold precursor concentration on the morphology and distribution of gold nanoparticles reduced on the PANI surface, two different $HAuCl_4$ concentrations, 1.8 mM and 0.36 mM, were investigated. The synthesized nanocomposites are listed in Table 1.

TGA analysis was performed on AuDT nanoparticles to estimate the mass fraction of the gold core compared to the 1-dodecanethiol coating, and the results are presented in Fig. 1a. As evident, the gold content in the nanoparticles is

Table 1 List of the synthesized PANI/Au hybrid nanocomposites

PANI/Au nanosystems	PANI synthesis technique	Au synthesis technique
PANI BF/AuDT	Biphasic (PANI BF)	Gold/dodecanthiol (AuDT) self-assembly
PANI RM/Au 1.8 mM	Rapid mixing (PANI RM)	Gold reduction (Au)
PANI RM/Au 0.36 mM	Rapid mixing (PANI RM)	Gold reduction (Au)

approximately 83%. Furthermore, the curve is characterized by a single degradation step, located approximately at 250 °C, associated with the degradation phenomenon of the DT coating.[29] Regarding the CSA-doped PANI BF nanofibers, two primary steps characterize the degradation curve: the initial mass loss from 200 °C to nearly 400 °C is attributable to the degradation of CSA, while the final step occurs between 400 °C and 700 °C and it is likely due to the CSA-doped PANI BF degradation.[30,31] By subtracting the PANI/Au nanocomposite residual weight @800 °C from that of the PANI nanofibers at the same temperature, it is possible to estimate the gold content in the nanosystems, which in the case of PANI BF/AuDT is approximately 14.6%. Moreover, the TGA curves of PANI BF and PANI BF/AuDT demonstrate the absence of a change in profile shape, indicating that AuDT nanoparticles do not affect the degradation process of the PANI nanofibers.

Fig. 1b presents the TGA curves of PANI RM, PANI RM/Au 1.8 mM and PANI RM/Au 0.36 mM. As expected, the increase by an order of magnitude in $HAuCl_4$ leads to a substantial alteration in the gold nanoparticle content, which increases from 10.3% in PANI RM/Au 0.36 mM to 27.8% in PANI RM/Au 1.8 mM.

The gold content in the synthesized PANI/Au hybrid nanocomposites is summarized in Table 2.

Fig. 2a displays the TEM image of the AuDT nanoparticles, and an average size of approximately 3–5 nm was deduced by a relative size histogram of AuDT NPs (Fig. S1, ESI†). The nanofibers produced using these nanoparticles *via* a bottom-up synthesis exhibit a uniform distribution of gold on the surface of the PANI, as demonstrated in Fig. 2b.

In contrast, in the synthesis of gold nanoparticles, the direct reduction of a gold precursor onto the polyaniline (PANI) nanofibers reveals that the concentration of $HAuCl_4$ has a substantial effect on the size of the resulting nanoparticles.

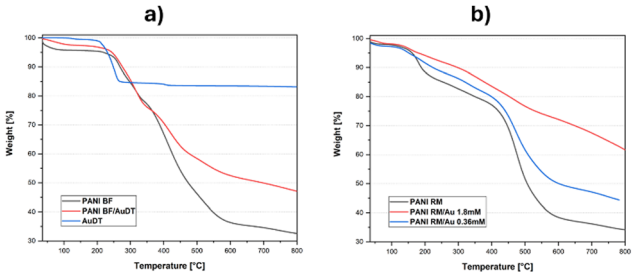

Fig. 1 TGA curves of (a) AuDT, PANI BF and PANI BF/AuDT as well as (b) PANI RM/Au.

Table 2 Gold content in PANI/Au nanocomposites

Nanocomposite system	Gold nanoparticle diameter [nm]	Gold content[a] [%]
PANI BF/AuDT	3–5	14.6
PANI RM/Au 1.8 mM	2–3	27.8
PANI RM/Au 0.36 mM	~1	10.3

[a] Evaluated by TGA; subtracting the PANI nanofiber residual weight @800 °C from that of the corresponding PANI/Au nanocomposite.

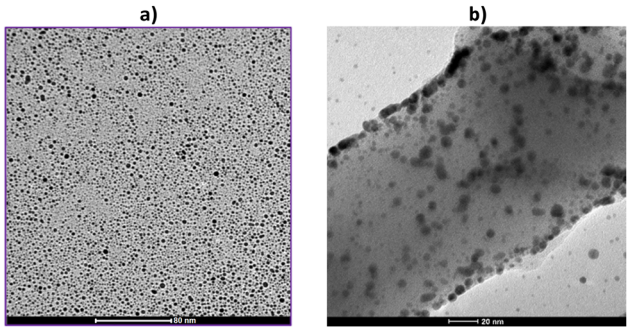

Fig. 2 TEM image of the synthesized (a) AuDT nanoparticles and (b) PANI BF/AuDT.

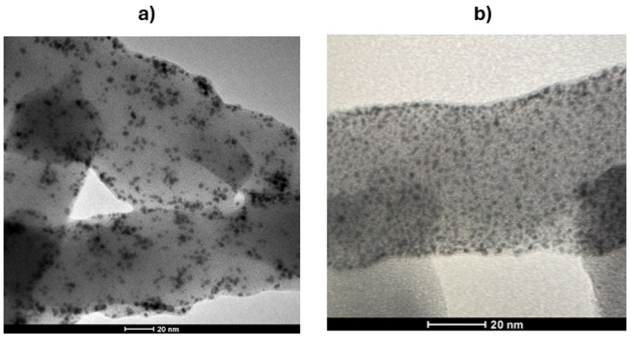

Fig. 3 TEM image of (a) PANI RM/Au 1.8 mM and (b) PANI RM/Au 0.36 mM.

This is clearly supported by the transmission electron microscopy (TEM) images shown in Fig. 3. In PANI BF/AuDT synthesis, AuDT particles are incorporated in the PANI fibers during their growth (localising them either into the fiber bulk and on the surface). On the contrary, in PANI RM/Au synthesis, gold nanoparticles nucleated almost exclusively onto the PANI fiber surface, which was already formed. In addition, a higher $HAuCl_4$ concentration will prompt the formation of larger nanoparticles (*i.e.*, diameter range of 2–3 nm), as confirmed by Fig. 3a. Conversely, the PANI RM/Au sample at a concentration of 0.36 mM exhibits comparatively smaller nanoparticles, as shown in Fig. 3b.

The TGA results and TEM observations suggest that the concentration of $HAuCl_4$ is a critical parameter for both the number and size of the synthesized gold nanoparticles.

3.2. Electrical characterization

The schematic layout of the fabricated devices is reported in Fig. 4a. The current–voltage (*I–V*) characteristics of these devices were systematically measured by a sequential direct current (DC) bias voltage protocol, which involved the application of voltages in the following order: 0 V, gradually increasing to 1 V (and 2 V specifically for the samples incorporating PANI BF/AuDT), followed by a decrease to −1 V (and −2 V for the PANI BF/AuDT samples), and concluding with a return to 0 V. The voltage was varied in discrete steps of 0.1 V throughout this process. These measurements were conducted using a Keithley 2400 Source Meter, with the positive voltage being applied to the bottom contact of the device.

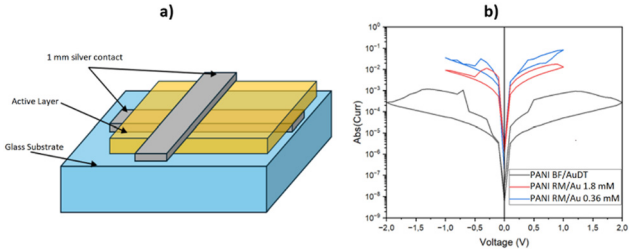

Fig. 4 (a) Schematic layout of the fabricated devices; (b) current–voltage characteristics (plot with absolute current) of the device with PANI BF/AuDT, PANI RM/Au 1.8 mM and PANI RM/Au 0.36 mM.

The *I–V* curves presented in Fig. 4b reveal that the investigated devices exhibit a typical and pronounced non-linear current–voltage curve characterized by the presence of a closed hysteresis loop. These results are indicative of a memristive-like behaviour, which implies that the devices are capable of exhibiting resistance changes that are influenced by their electrical history. According to Tseng *et al.*,[25] electrical resistance switching is attributable to the electric-field-induced charge transfer between the conjugated polyaniline and gold nanoparticle. Moreover, as reported by Li *et al.*,[8] the control tests have revealed that the memristive effect is closely related to the PANI/gold junction because the presence of only one of the two will make this effect disappear.

Such memristive behaviour is of significant interest in the field of neuromorphic computing and memory devices, suggesting the potential for applications in non-volatile memory storage and processing capabilities. Further analysis indicates that the devices fabricated using nanofibers obtained through rapid mixing techniques demonstrate conductivities that are nearly two orders of magnitude greater than those derived from the biphasic synthesis method.

The difference in the current and hysteresis shape is attributable to the structure and sizes of the gold nanoparticles. Firstly, in the case of PANI BF/AuDT, the current is reduced at the same bias value due to the presence of an organic shell (DT) onto the gold nanoparticles acting as a charge transfer barrier. In PANI RM samples, the curve profiles are similar with an increased current density, as in the case of PANI RM/Au 0.36 mM. This latter evidence is likely due to the smaller gold particles uniformly distributed onto the PANI fiber surface, which enhance the contact surface, and thus, the conductivity between the metal and the polymer. This substantial difference in conductivity is critical, as it influences the operational voltage range of the devices. Consequently, for the devices produced *via* rapid mixing, the voltage sweep was deliberately limited to a maximum of 1 V to prevent potential damage or undesired effects due to excessive current flow. In contrast, the devices produced with nanofibers from the biphasic synthesis process could tolerate higher voltage sweeps, necessitating the application of voltages up to 2 V. The stability and reproducibility of the observed *I–V* curves upon repeated cycling (Fig. S2–S4, in ESI†) further emphasizes the reliability of the memristor-like behaviour exhibited by the devices. Such a feature is fundamental

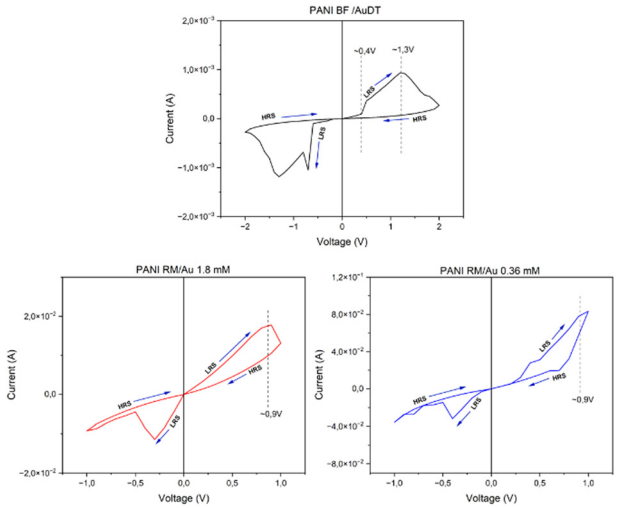

Fig. 5 Hysteresis loops exhibited by the three devices, indicating two states: high resistance state (HRS) and low resistance state (LRS).

for practical applications, as it indicates that the devices can maintain consistent performance over time, which is a crucial attribute for any memory or processing device for real applications.

Fig. 4 reports that the analysed devices exhibit characteristics associated with memristive-like behaviour. Specifically, the resistance of these devices is not a fixed property but is dependent upon the applied history of voltage and current, underscoring the potential utility of these devices in advanced memory technologies and neuromorphic systems. The findings suggest that optimizing the synthesis methods for nanofibers could significantly enhance device performance, paving the way for future research and development in this area.

Fig. 5 clearly shows evidence for the transition of memristors from a low resistance state (LRS) to a high resistance state (HRS) in response to the increasing applied voltage. Samples produced with the "rapid mixing" method switch from LRS to HRS at a lower voltage ($\sim$0.9 V) compared to those made using the "biphasic synthesis" method ($\sim$1.3 V).

A further notable observation is related to the behaviour of these devices under negative voltage conditions. In fact, as the applied voltage is inverted and decreases, the device reverts to its initial LRS. This indicates that, upon exceeding a specific negative threshold voltage, the device operates a back-transition to the high resistance state, suggesting that it can retain its previous state upon the power removal. This specific characteristic categorized these devices as volatile memristors and it induces substantial implication at the scientific level and in practical technological applications, implying operational characteristics under differing electric field conditions.[32]

4. Conclusions

This work described two distinct synthetic routes for preparing conductive PANI/Au hybrid nanocomposites, finding significant differences in their morphology and electrical properties. The major effects of the fabrication technique on the

performance of the final product were demonstrated for the hybrid composites prepared by rapid mixing, which revealed higher conductivity compared to those attained by the biphasic synthesis procedure.

Demonstrating the ability of these devices to effectively switch states in response to the applied voltage is fundamental for potential applications in memory technology, advanced sensors, flexible electronics and neuromorphic computing systems. Further optimization will be performed in the fabrication conditions to improve the conductive properties and scalability of PANI/Au-based nanocomposites at the voltage thresholds.

Author contributions

Conceptualization A. B., A. C., M. M.; experiments A. Z., S. A., A. R.; methodology and data analysis A. Z., S. A., A. R., M. Z.; reference investigation, A. Z., S. A.; data curation A. Z., S. A., S. Z., A. R.; writing – original draft preparation All; writing – review and editing, All; supervision, A. B., A. C., M. Z., P. T. All authors have read and agreed to the published version of the manuscript.

Data availability

The data supporting this article have been included as part of the ESI.†

Conflicts of interest

There are no conflicts to declare.

Acknowledgements

The authors thank Ms Mariacristina Del Barone for the technical support in SEM analysis.

References

1 C. W. Chu, J. Ouyang, J. H. Tseng and Y. Yang, *Adv. Mater.*, 2005, **17**, 1440.
2 C. P. Collier, E. W. Wong, M. Belohradský, F. M. Raymo, J. F. Stoddart, P. J. Kuekes, R. S. Williams and J. R. Heath, *Science*, 1999, **285**, 391.
3 S. W. Lee, C. Mao, C. E. Flynn and A. M. Belcher, *Science*, 2000, **296**, 892.
4 R. J. Tseng, J. Huang, J. Ouyang, R. B. Kaner and Y. Yang, *Nano Lett.*, 2005, **5**, 1077.
5 C. O. Baker, X. Huang, W. Nelson and R. B. Kaner, *Chem. Soc. Rev.*, 2017, **46**, 1510.
6 P. Chandrasekhar, *Conducting Polymers, Fundamentals and Applications: A Practical Approach*, Kluwer Academic Publishers, Boston, MA (1999).
7 A. G. MacDiarmid, J. C. Chiang, A. F. Richter and A. J. Epstein, *Synth. Met.*, 1987, **18**, 285.
8 N. R. Chiou and A. J. Epstein, *Adv. Mater.*, 2005, **17**, 1679.
9 Y. Wang, *Poly. Int.*, 2018, **67**, 650–669.
10 K. L. Kelly, E. Coronado, L. L. Zhao and G. C. Schatz, *J. Phys. Chem. B*, 2003, **107**, 668.
11 J. Han, M. Wang, Y. Hu, C. Zhou and R. Guo, *Prog. Polym. Sci.*, 2017, **70**, 52–91.
12 A. Thomas, *J. Phys. D: Appl. Phys.*, 2013, **46**, 093001.
13 M. Li, Y. Guo, Y. Wei, A. G. Macdiarmid and P. I. Lelkes, *Biomaterials*, 2006, **27**, 2705.
14 C. G. Wu and T. Bein, *Science*, 1994, **264**, 1757.
15 W. Zhong, J. Deng, Y. Yang and W. Yang, *Macromol. Rapid Commun.*, 2005, **26**, 395.
16 A. Abdolahi, E. Hamzah, Z. Ibrahim and S. Hashim, *Materials*, 2012, **5**, 1487.
17 X. Zhang, W. J. Goux and S. K. Manohar, *J. Am. Chem. Soc.*, 2004, **126**, 4502.
18 Z. A. Boeva and V. G. Sergeyev, *Polym. Sci.*, 2014, **56**, 144.
19 K. A. Milakin, A. N. Korovin, E. V. Moroz, K. Levon, A. Guiseppi-Elie and V. G. Sergeyev, *Electroanalysis*, 2013, **25**, 1323.
20 Y. G. Wang, H. Q. Li and Y. Y. Xia, *Adv. Mater.*, 2006, **18**, 2619.
21 J. Huang and R. B. Kaner, *J. Am. Chem. Soc.*, 2004, **126**, 851.
22 S. K. Pillalamarri, F. D. Blum, A. T. Tokuhiro and M. F. Bertino, *Chem. Mater.*, 2005, **17**, 5941.
23 T. K. Sarma, D. Chowdhury, A. Paul and A. Chattopadhyay, *Chem. Commun.*, 2002, 1048.
24 R. J. Tseng, C. O. Baker, B. Shedd, J. Huang, R. B. Kaner, J. Ouyang and Y. Yang, *Appl. Phys. Lett.*, 2007, **90**, 053101.
25 J. Ouyang, C. Chih-Wei, C. R. Szmanda, L. Ma and Y. Yang, *Nat. Mater.*, 2004, **3**, 918.
26 A. Borriello, P. Agoretti, A. Cassinese G. T. Mohanraj and L. Sanguigno. EP2136421B1 (17/06/2008) New synthesis of hybrid polymer-metal nanostructures and hybrid polymer-metal compounds nanostructures for nanodevice applications.
27 D. Li and R. B. Kaner, *J. Am. Chem. Soc.*, 2006, **128**, 968–975.
28 J. Han, L. Li and R. Guo, *Macromolecules*, 2010, **43**, 10636.
29 F. Locardi, E. Canepa, S. Villa, I. Nelli, C. Lambruschini, M. Ferretti and F. Canepa, *J. Anal. Appl. Pyrolysis*, 2018, **132**, 11.
30 W. Li and M. Wan, *J. Appl. Polym. Sci.*, 1999, **71**, 615.
31 R. S. Biscaro, M. C. Rezende and R. Faez, *Poly. Adv. Technol.*, 2009, **20**, 28.
32 Y. Yu, M. Xiao, D. Fieser, W. Zhou and A. Hu, *J. Mater. Chem. C*, 2024, **12**, 3770.